Linear Simulation of the Stationary Eddies in a GCM. Part II: The "Mountain" Model

SUMANT NIGAM

Department of Earth, Atmospheric and Planetary Sciences, Massachusetts Institute of Technology, Cambridge, Massachusetts

ISAAC M. HELD AND STEVEN W. LYONS*

Geophysical Fluid Dynamics Laboratory/NOAA, Princeton, New Jersey

(Manuscript received 30 June 1987, in final form 3 November 1987)

ABSTRACT

The validity of linear stationary wave theory in accounting for the zonal asymmetries of the winter-averaged tropospheric circulation obtained in a general circulation model (GCM) is ascertained. The steady linear primitive equation model used towards this end has the same vertical and zonal resolution as the spectral GCM, but is finite-differenced in the meridional direction. It is linearized about a zonally symmetric basic state and forced by topography and 3-dimensional diabatic heating and transient flux convergence fields, all of which are taken from the GCM. As in Part I, (in which we studied a GCM with a flat lower boundary) we obtained the best correspondence between the GCM and the linear solutions when strong Rayleigh friction is included in the linear model not only near the surface, but in the interior of the tropical troposphere as well.

There is sufficient quantitative correspondence between the GCM and the linear solution to justify decomposing the linear simulation into parts forced by different processes, although in some regions, such as over North America, the simulation is unsatisfactory. Different fields give different impressions as to the relative importance of orography, heating, and transients. The eddy zonal velocity field in the upper troposphere shows the orographic and thermal plus transient contributions to be nearly equal in amplitude, whereas the eddy meridional velocity field, dominated by shorter zonal scales, shows the orographic contribution to be decisively dominant. Although there is no systematic phase relationship between these two contributions, they are roughly in phase over the east Asian coast, where each of them is largest. They also contribute roughly equal amounts to the low level Siberian high.

Other findings are that (i) the 300 mb extratropical response to tropical forcing reaches 50 gpm over Alaska (given our frictional parameterization), which is smaller than the response to local thermal forcing, (ii) the responses to sensible heating and lower tropospheric thermal transients are strongly anticorrelated, and (iii) the circulation in the vicinity of the Andes in the GCM is not attributable to direct mechanical forcing by the mountains.

1. Introduction

In Nigam et al. (1986, hereafter referred to as I), the validity of linear stationary wave theory is examined by comparing the solutions of a linear primitive equation model on the sphere with the thermally forced stationary eddies produced by a general circulation model (GCM) having a flat surface. In this paper we describe a similar comparison, but for a model that has realistic orography. The questions we ask here are similar to those in I.

- To what extent is the linear theory qualitatively, or even quantitatively valid?
- What are the roles played by different orographic features, diabatic heating and transient eddy flux convergences in forcing different aspects of the stationary eddy pattern?
- Can a linear model in which the singularity at critical latitudes is removed by adding damping (so that waves incident on these layers are efficiently absorbed) simulate the GCM's eddies, or are there signs of significant reflection in the GCM?
- To what extent is it desirable to include other dissipative terms (Rayleigh friction, Newtonian damping, diffusion) not only to remove any singularities in the linear dynamics, but to parameterize processes that are not includable in such linear models?

The central importance of orographic forcing for the stationary wave pattern during Northern Hemisphere winter has been recognized since the work of Charney and Eliassen (1949). Debate on the relative importance of orographic and extratropical thermal forcing began immediately (e.g., Sutcliffe, 1951; Smagorinsky, 1953)

* Present affiliation: Department of Meteorology, Texas A & M University, College Station, TX 77843.

Corresponding author address: Dr. Sumant Nigam Center for Ocean-Land-Atmosphere Interactions, Department of Meteorology, University of Maryland, College Park, MD 20742.

and continues unabated. Recent work has also highlighted the potential importance of tropical heating (e.g., Webster, 1982; Simmons, 1982; Jacqmin and Lindzen, 1985) and of mixing by large-scale transients (e.g., Youngblut and Sasamori, 1980; Opsteegh and Vernekar, 1982). In addition, implicit in much of the work on multiple equilibria for stationary waves (beginning with Charney and DeVore, 1979) is the possibility that the climatological stationary eddies, being an average over dissimilar quasi-steady states, may not have a simple dynamic explanation.

There have been two major approaches to analyzing the forcing of stationary eddies by orography: (i) linear stationary wave models; and (ii) the comparison of GCM simulations obtained with and without orography. The first of these approaches has a longer history. A discussion of the limitations of many of the earlier beta-plane channel models, primarily due to the distortions caused by the artificial walls, can be found in Held (1983). Examples of more recent multilayer linear primitive equation models with spherical geometry are Hoskins and Karoly (1981), Simmons (1982), Hendon and Hartmann (1982), Lin (1982) and Jacqmin and Lindzen (1985). The first and the last of these papers, in particular, discuss the response to realistic orography and various types of extratropical and tropical thermal forcings. As discussed in I, in such studies one is never sure whether the discrepancies between linear model solutions and observations are due to breakdown of the steady linear model or inadequately defined forcing or both. Uncertainty in the three-dimensional distribution of the climatological diabatic heating field is particularly troubling.

The GCM calculations with and without mountains are in one sense more straightforward. While one must keep the model limitations in mind, to the extent that the model produces a good simulation of the stationary eddies one has a direct measure of the total effect of orography on the zonal asymmetries. One cannot, however, easily separate this total effect into a part due to the direct mechanical effect of orography and a part forced by changes in diabatic heating and transient eddy flux convergences that result due to the presence of orography. Indeed, only to the extent that a linear model of the stationary eddies is successful is a separation of this sort meaningful. GCM calculations with and without mountains have been discussed by Kasahara and Washington (1971), Manabe and Terpstra (1974), Held (1983), Tokioka and Noda (1986), and Blackmon et al. (1987). There are substantial differences among the different model results. For example, Manabe and Terpstra, Held, and Tokioka and Noda all show a large (>10 m s^{-1}) weakening of the zonal wind maximum off the coast of Asia when mountains are removed from the model, while the other two studies do not. All of the models agree that "thermal" forcing is of greater importance for the largest zonal scales in the upper troposphere, particularly wavenumber 1. Another common finding, which historically has also been deduced from a comparison of the observed wintertime and summertime stationary waves, is that "thermal" forcing tends to dominate near the surface.

As in I, we try to combine the virtues of these two approaches by simulating the results of GCM calculations with a linear primitive equation model on the sphere that is linearized about the GCM's zonally averaged flow, and forced with the GCM's orography, heating and transient eddy fluxes. The GCM used in this study is of low horizontal and vertical resolution; it has a rhomboidal truncation at wavenumber 15 in the horizontal and has nine sigma levels in the vertical. However, in most respects, the differences between the "mountain" model simulations described here and the "no-mountain" model simulations of I are similar to those obtained from the use of a higher resolution gridpoint GCM in Manabe and Terpstra (1974).

We have studied the low resolution GCM as it can be run for extended periods (15 years in this case), and this allows the model's climatology as well as its interannual variability to be quite well defined. One can analyze both the climatology and the interannual variability of the GCM circulation using a steady linear primitive equation model, but here we restrict ourselves to analyzing the wintertime stationary eddies alone. Lau (1983) discusses the dominant patterns of low-frequency variability seen in this same GCM integration. Linear simulations and diagnoses of the interannual variability in the GCM circulation will be reported elsewhere.

The steady linear model, the zonally symmetric basic state about which the model is linearized, the forcing functions, and the method of solution are all briefly described in section 2. The adequacy of linear stationary wave theory in explaining the seasonally averaged tropospheric circulation during Northern Hemisphere winter is examined in section 3 by comparing the steady linear solutions with the GCM solutions, and with Oort's (1983) diagnoses of the wintertime atmospheric circulation; Section 3 also contains evaluations of the relative importance of Eastern and Western hemispheric orographies, and of tropical and extratropical thermal plus transient forcings. In section 4, the upper tropospheric response to diabatic heating plus thermal and mechanical transients is split into tropically and extratropically forced parts; each of these is then decomposed further. The sensitivity of the steady linear solutions to thermal and mechanical damping processes is discussed in section 5. Discussion and conclusions follow in section 6.

2. The linear model and forcing functions

The steady linear primitive equation model is described in detail by Nigam (1983). While the model allows one to retain the mean meridional circulation in the basic state about which one linearizes, we do

not take advantage of this feature here and therefore set $\bar{V} = \bar{\sigma} = 0$. The stationary eddy pattern is calculated in σ-coordinates. For dynamical interpretation it is preferable to present results in pressure coordinates, but there is some uncertainty in defining the best way to compare linear solutions with GCM's in regions of high orography, such as the Tibetan plateau. Our procedure is to add the predicted stationary eddy to the mean flow in σ-coordinates, interpolate the total field to pressure levels, and then remove the zonal mean on these pressure surfaces. All forcing functions entering the linear model are first multiplied by a small number d, so as to avoid losing information in regions where surface pressure would otherwise be smaller than the pressure at which we examine the response. The final stationary eddy pattern in pressure coordinates is then multiplied by d^{-1}. The zonal mean zonal flow about which we linearize is taken from the "Mountain GCM", and as shown in Fig. 1a, it has tropical easterlies only in the lower troposphere ($p > 600$ mb). It is very similar to the zonal mean zonal flow obtained from the "No Mountain GCM" (see Fig. 1a in I); topographically forced stationary waves have little impact on the time-mean zonally averaged flow, at least in this GCM.

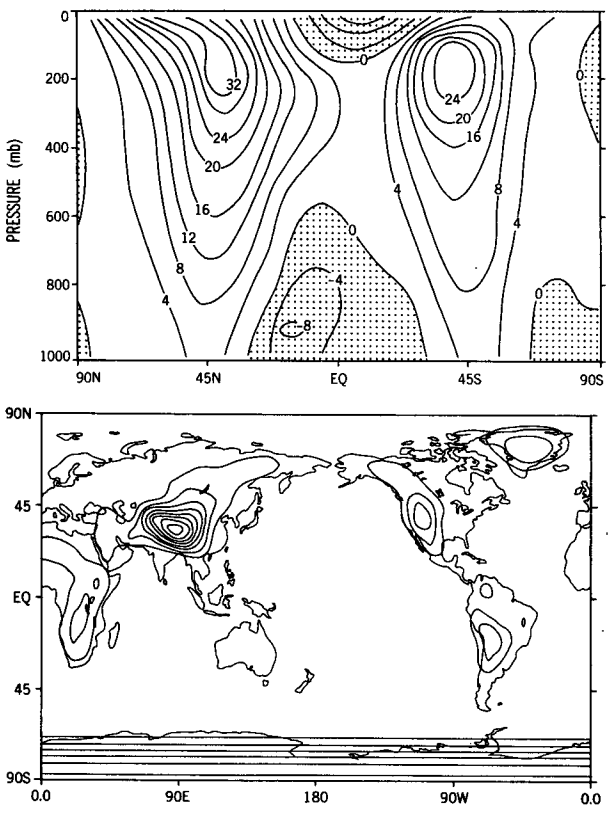

FIG. 1. The upper part shows the latitude–pressure plot of the wintertime zonally averaged zonal wind as obtained from the Mountain GCM and used as the basic state in the linear model, in m s^{-1}, and with easterlies shaded. The lower part shows the total (sum of the eddy and zonal mean components) orography used in the linear model; the contour interval is 500 m and the zero contour is not shown (the eddy topography south of 65°S is set equal to zero).

The linear model and the GCM use identically smoothed orography everywhere except over Antarctica ($\theta < 65$°S) where we set the linear model eddy orography to zero. We find that the solution in the Southern Hemisphere deterioriates when Antarctica is included, which is not particularly surprising given the nonlinear character of the flow around this steep ice-sheet. In contrast, the orography of Greenland has little impact on the linear model solutions and is thus retained in our calculations. (Rong-hui and Gambo, 1982, show a large contribution from Greenland in their orographic response, presumably due to the use of a stronger basic state flow near the surface in high latitudes). The total orography (with the eddy component over Antarctica removed) is shown in Fig. 1b. In the Himalayan–Tibetan complex, the maximum height is in excess of 4000 m whereas over the Rockies heights exceed 1500 m; a large area of the Greenland plateau has an elevation of well over 1000 m. Linear theory predicts that amplitudes of stationary Rossby waves generated by a localized topographic feature are sensitive only to the volume of that feature, and so a standard smoothing algorithm that more or less conserves volume should not have a dramatic effect on the forced linear response; the full nonlinear model may, however, be more sensitive to such orographic smoothing.

Figure 2a is a plot of the climatological wintertime-mean vertically averaged heating rate due to diabatic effects as well as transient eddies in the model. This total heating rate is then divided into contributions from latent heating (Fig. 2b), sensible heating plus radiative heating (Fig. 2c), and transients (Fig. 2d). The zonal mean of the heating rate has been removed in all cases. The clouds in this GCM are prescribed to be zonally symmetric and this minimizes any influence of radiative heating in forcing stationary eddies in the GCM. The zonally asymmetric component of sensible plus radiative heating (shown in Fig. 2c) is almost entirely due to sensible heating.

Comparison with Fig. 2 in I shows the changes in heating rates due to the presence of mountains. One significant change is that the storm track heating off the Asian coast is more intense (by at least 1°K day^{-1}) and extends further equatorward in the "Mountain GCM", as also in Manabe and Terpstra (1974); this results from comparable increments in latent and sensible heating that are largely in phase over this region. Modulation of the storm track heating over the Atlantic is more modest. Another significant change in the Mountain GCM total heating field is the localized heating over the Tibetan plateau. It is not clear how best to treat such an elevated heat source in our linear model. We simply take the heating rate per unit mass as a function of σ from the GCM and utilize it directly

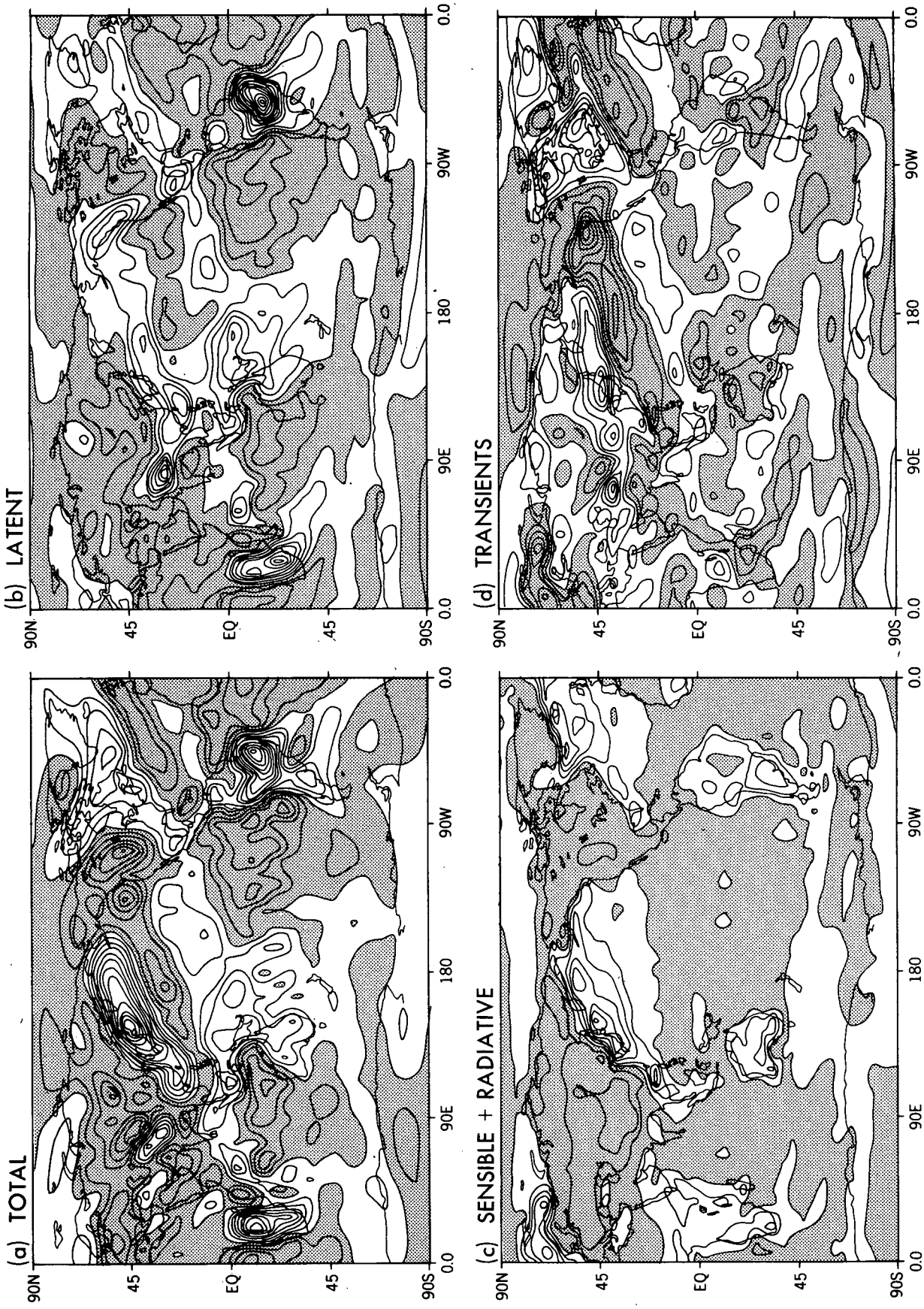

FIG. 2. Vertically averaged heating rates for the Mountain GCM's wintertime simulation, with the zonal mean removed, contour interval 0.25°K day^{-1}, and negative values shaded: (a) total heating, (b) latent heat release, (c) sensible plus radiative heating; and (d) heating due to transients.

in the linear model, ignoring the fact that this results in too large a vertically integrated heating rate over Tibet. Compounding the problem, this localized heating over the Tibetan plateau is at least partly due to truncation errors in the σ-coordinate moisture equation in this low-resolution spectral GCM (S. Manabe, personal communication).

The compensation between extratropical sensible heating and transients noted in I is also evident here. Clear examples are found over and south of Greenland and over Scandinavia. Given this compensation, one suspects that division of the stationary wave field into parts forced separately by diabatic heating and lower tropospheric transients (which dominate the vertically averaged transient heating shown in Fig. 2d) may not be particularly informative.

There are significant differences in the tropical heating rates between the Mountain and No-Mountain GCMs. In particular, latent heating over South America and Africa is much more intense in the Mountain model; heating over Indonesia is also somewhat stronger. We suspect that most of these changes in the tropical precipitation pattern are related to the local relief within the tropics, rather than to the extratropical orography. The Indonesian heating appears to be weak in this model (cf. the heating estimates in Johnson et al., 1985). As found in I, the heating by transients in the tropics is not entirely negligible and tends to attenuate the total thermal forcing of the stationary eddies.

Estimates of the contribution of thermal and mechanical transients and stationary nonlinearities to the forcing of the stationary waves are complicated by the necessity of removing the singularity in a linear inviscid stationary wave model at points where the mean zonal wind $\bar{U}$ vanishes. In the calculations described below, we use precisely the same damping mechanisms as in I: 1) a Rayleigh friction in the momentum equations (ϵ_c) that is a function of $\bar{U}$ [see Eq. (1b) in I]; because $\bar{U}$ in Fig. 1a is very similar to that in I, the latitude-height structure of ϵ in this calculation is nearly the same as depicted in Fig. 1b of I, and has a maximum value of $(1.5 \text{ days})^{-1}$ in regions where $\bar{U}$ vanishes; 2) an additional Rayleigh friction (ϵ_b) near the surface to represent boundary layer stresses; and 3) a small linear diffusion of momentum and temperature. The linear diffusion generally has a very minor effect on larger scales of the linear responses, but it does damp small-scale noise in some of the results. We also describe a calculation in which simple thermal damping is included when calculating the response to orography in the linear model. In the absence of thermal damping, the linearized thermodynamic equation is inviscid except for the small diffusion term, and this results in deterioration of the low-level solutions near the transition from subtropical westerlies to easterlies, just as in I. We believe that this problem is related to the awkwardness in treating low-level heat fluxes as a prescribed forcing, since they are diffusive in character and strongly controlled by stationary waves themselves.

The Rayleigh friction that comes into play when $\bar{U}$ is small, and which should be thought of as representing the effect of nonlinearities, is of central importance to the simulation within the tropics. As described in I, the linear model requires large damping (larger than what is needed for removing the singularity of linearized dynamics at the prescribed model resolution) to produce a realistic magnitude for the tropical stationary eddies forced by tropical heating. The fact that the same frictional parameterizations yield useful linear model simulations both in I and in the present case increases our confidence in this approach. It is an important problem to determine the extent to which nonlinear stationary models are capable of producing similar (or better) results with smaller or less arbitrary tropical momentum damping.

3. The steady linear responses

The stationary waves resulting from our linear simulations are summarized in Figs. 3–6. Figures 3 and 4 contain latitude–longitude plots of the stationary eddy zonal and meridional velocities at 300 mb (with a 4 m s^{-1} contour interval for U' and 2 m s^{-1} for V'). Figure 5 contains polar stereographic projections of the NH eddy geopotential height at 300 mb (with a 40 gpm contour interval), and Fig. 6 is an analogous figure for the 900 mb level (with a 20 gpm contour interval).

There are six frames in each of these figures: (a) the GCM stationary eddy field averaged over 45 winter months from 15 simulated winters; (b) the corresponding observed winter season (DJF) field, obtained from Oort's (1983) data analyses, (c) the total linear model solution; (d) the linear response to diabatic heating plus transient forcing[1]; (e) the linear response to orography; and (f) the difference between the stationary eddies simulated by the Mountain GCM and those simulated by the No Mountain GCM. The sum (d) + (e) equals (c), which is to be compared with (a). The comparison of (e) and (f) tests not only the linearity of the mechanical response to orography, but also whether mechanically forced waves dominate over changes in thermally forced waves that occur due to the presence of orography in the GCM.

The stationary eddies simulated in the GCM resemble those in the atmosphere sufficiently closely, in our view, that the understanding we gain of the GCM should be of value in understanding the atmosphere as well. In comparing the GCM and the observations in Figs. 3–6 one must keep in mind the data analysis interpolation errors in rawinsonde-sparse regions (see Figs. 3b and 4b in Oort (1983) for the distribution of data points). This is a significant problem in the eastern tropical Pacific (where Newell et al. (1974), for example, have much stronger equatorial westerlies) and in much of the Southern Hemisphere, but even in the Northern

[1] The transience in the $\ln p_s$ equation is ignored in these calculations.

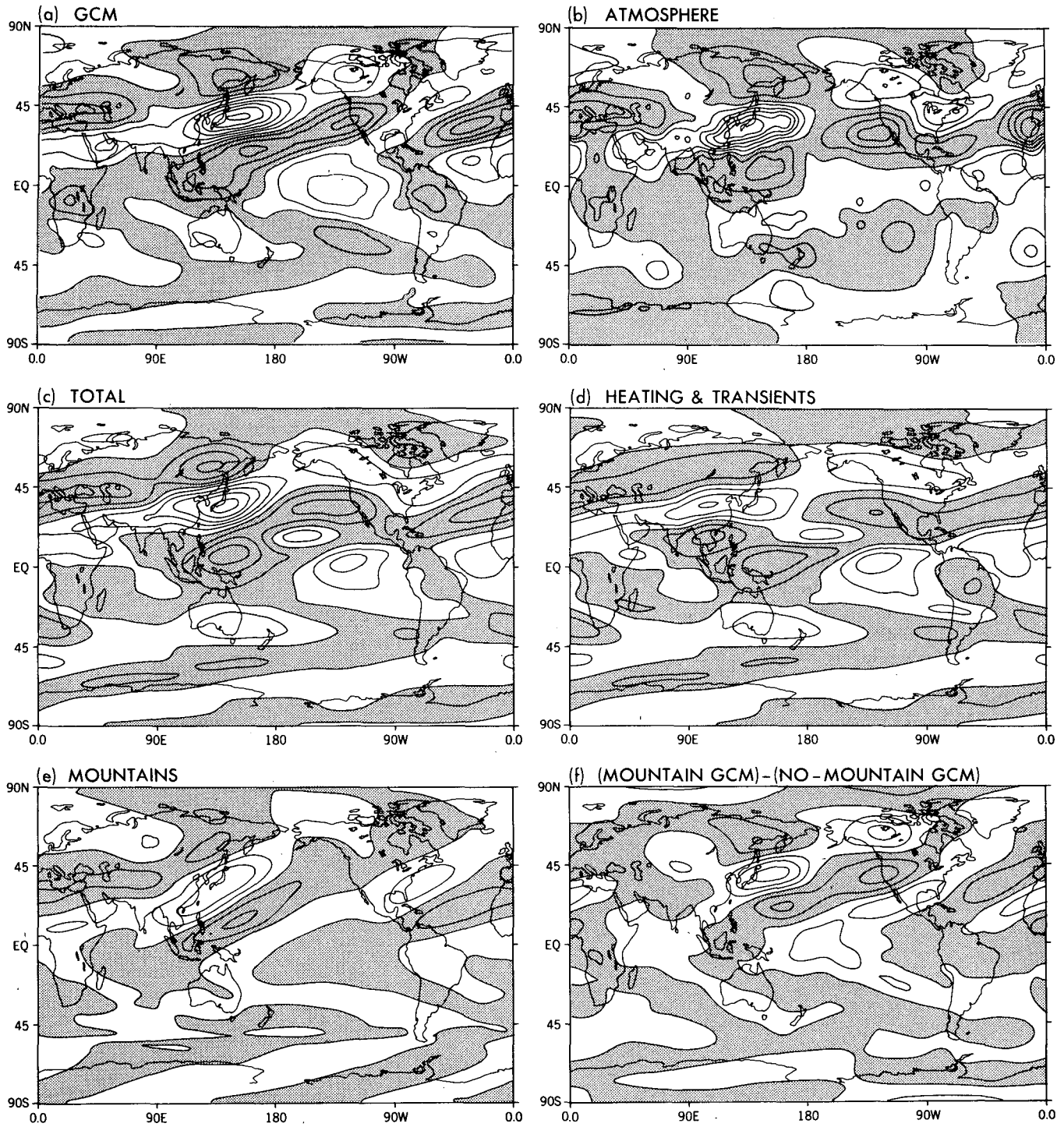

FIG. 3. The 300 mb eddy zonal velocity field is shown with a contour interval of 4 m s^{-1} and with negative values shaded: (a) the Mountain GCM's winter climate, (b) Oort's (1983) analysis of wintertime observations, (c) the total linear model solution, (d) the linear response to diabatic heating plus transient (thermal and mechanical) forcing, (e) the linear response to orography, and (f) the difference between the wintertime circulation of the Mountain and the No Mountain GCM.

Hemisphere one must be wary of data reliability over the oceanic jet-exit regions (see Lau and Oort, 1981). It is noteworthy that the GCM's eddy zonal wind at the jet maximum off Japan, where the data should be adequate, is of nearly the correct magnitude, despite the fact that the Indonesian heating appears to be weak. On the other hand, the jet maximum off the North American east coast is definitely too weak, as are the

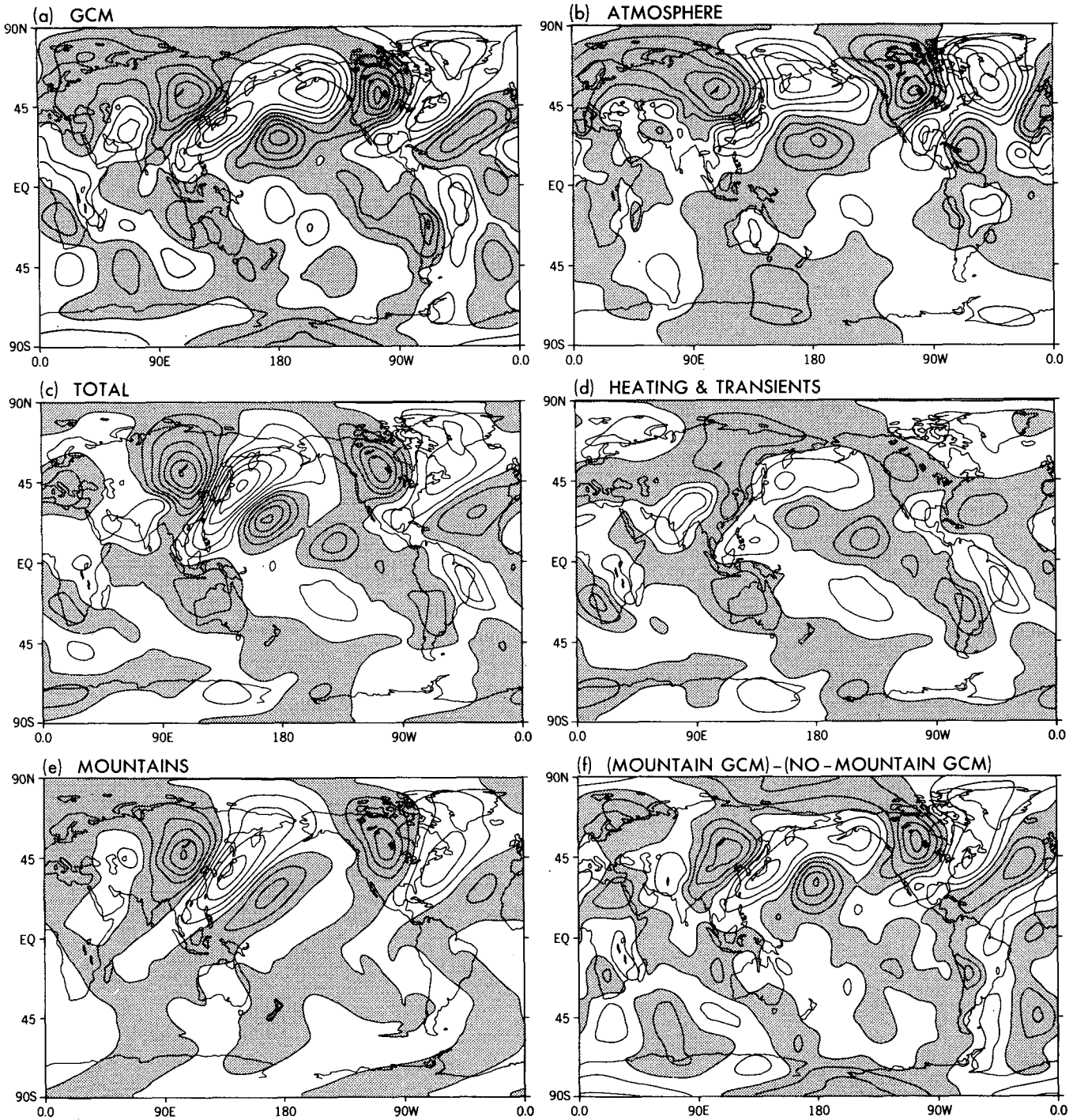

FIG. 4. As in Fig. 3 except for the 300 mb eddy meridional velocity; the contour interval is now 2 m s^{-1}.

associated upper tropospheric low over North America and high over Europe (Fig. 5). The 900 mb low over eastern Canada is also too weak (Fig. 6).

Figure 3 shows that orography and heating plus transients are of comparable importance in the linear simulation of the 300 mb perturbation zonal wind. The linear model produces a 21 m s^{-1} perturbation zonal wind maximum off Japan at 300 mb when forced by topography, heating, and transients, as compared with 25 m s^{-1} in the GCM. Orography alone produces a jet maximum at the same position as that in the full linear model, but of amplitude 11 m s^{-1}; heating plus transients contribute the remaining 10 m s^{-1}. The Indonesian region easterlies equatorward of this jet are

not as well simulated by the linear model, although their amplitude is approximately correct. In the linear model, the wavetrain emanating from Tibet produces an easterly maximum of -9 m s^{-1} at 10°N, while heating plus transients force two easterly maxima in this region, one centered on the equator and another over Indochina.

The tropical perturbation westerlies in the eastern Pacific have the correct amplitude as compared with the GCM, and are entirely forced by heating plus transients. However, the linear solution in the subtropical Pacific has exaggerated meridional structure. On the other hand, the zonal wind structure over the North Atlantic is simulated reasonably well by the full linear model, and is produced by nearly in phase superposition of orographic and thermal plus transient parts. The amplitude of the total linear solution is underestimated in the southern subtropics, e.g., over the Congo and the Amazon basins, and, perhaps, a little overestimated over the remaining Southern Hemisphere. Such discrepancies between the linear and the GCM solution may result from the particular choice of meridional structure of the Rayleigh friction coefficient in the tropics.

The 300 mb perturbation meridional velocity (Fig. 4) gives a different impression as to the relative importance of orography and heating plus transients. The full linear simulation agrees well with the GCM in most regions, in amplitude as well as in phase (the most significant discrepancy being over Alaska), and at least three-quarters of the amplitude in midlatitudes is accounted for by the orographic forcing. Separate wavetrains emanating from Tibet and the Rockies are again evident, although the ray paths that dominate the V' field are more zonally oriented than those dominating the U' field, as expected from the transverse character of Rossby waves. Notice that tropical heat sources drive a circulation that is about twice as strong in the zonal plane as in the meridional plane. The solution over South America is forced by heating plus transients and not by the direct mechanical forcing due to the Andes (cf. Kalnay et al., 1986). Comparison of Figs. 4e and 4f shows however that both the Andes and the African topography do affect the local circulation indirectly by modifying the heating and transients. This comparison also indicates that the wavetrain generated by the Rockies in the linear model is attenuated a bit too strongly as it enters the tropics and that its ray path is also somewhat distorted.

The Northern Hemisphere 300 mb geopotential (Fig. 5) shows that the low off the coast of Asia in the linear model is positioned slightly to the west of its position in the GCM and is slightly too strong (by about 20 gpm), while the low in the lee of the Rockies is significantly stronger, and the high upstream of the Rockies considerably weaker, than in the GCM. There is also an anomalous high in the linear model over northwest Russia. However, overall there is a remarkable degree of similarity between the full linear model and the GCM (except over the North American continent), confirming that linear stationary wave theory is a useful starting point for analyzing climatological zonal asymmetries.

The 300 mb geopotential gives an impression as to the relative importance of orography and heating plus transients that is half way between those given by the decomposition of the U' and V' fields. Orography directly forces two-thirds of the dominant low off the Asian coast. Heating plus transients force a low at nearly the same location but of roughly half the amplitude. There is constructive interference between orographic and heating plus transient forcing also in the highs off the western coast of North America and over Europe, but destructive interference in the region of the low over central and eastern North America. The anomalous high over Northern Russia is forced by heating plus transients.

Our linear topographic response at 300 mb is similar to that of Jacqmin and Lindzen's (1985, see Fig. 5b in their paper) except in the western hemisphere where Jacqmin and Lindzen's amplitudes are at least 50% larger than ours: the most notable discrepancy being in the simulation of the Aleutian anticyclone which in their solution is not only much too strong but also incorrectly placed. Our solution is also different from that of Hoskins and Karoly (1981) who obtain comparable amplitudes but smaller wavelengths and more poleward directed wavetrains in their calculations with realistic orography (presumably caused by differences in the basic state flow). Except over the Himalayas, there is also a striking similarity between this baroclinic solution and the barotropic response to the same topography shown in Fig. 6.8a of Held (1983). The barotropic response was obtained by setting the stretching in the vorticity equation equal to

$$\frac{f}{H}\frac{\bar{U}_s}{a\cos\theta}\frac{\partial h'_T}{\partial \lambda}$$

where $\bar{U}_s$ is the mean surface wind, H the scale height, and h'_T the eddy orography; the resulting amplitudes are smaller than those in Fig. 5e by a factor of 3 or so. To the extent that the barotropic response is dominated by external Rossby waves, the factor by which such a barotropic model underestimates the true linear response at the equivalent barotropic level (which is below 300 mb) can be computed. This factor is denoted by α_s in Held et al. (1985), and was estimated to be about 2.

Figure 6 shows the 900 mb eddy geopotential response to heating plus transients to be comparable and occasionally larger than the response to orography. The Aleutian low is weak and displaced westward as compared with the GCM and observations. The decomposition into parts forced by heating plus transients and mountains gives the impression that the reason

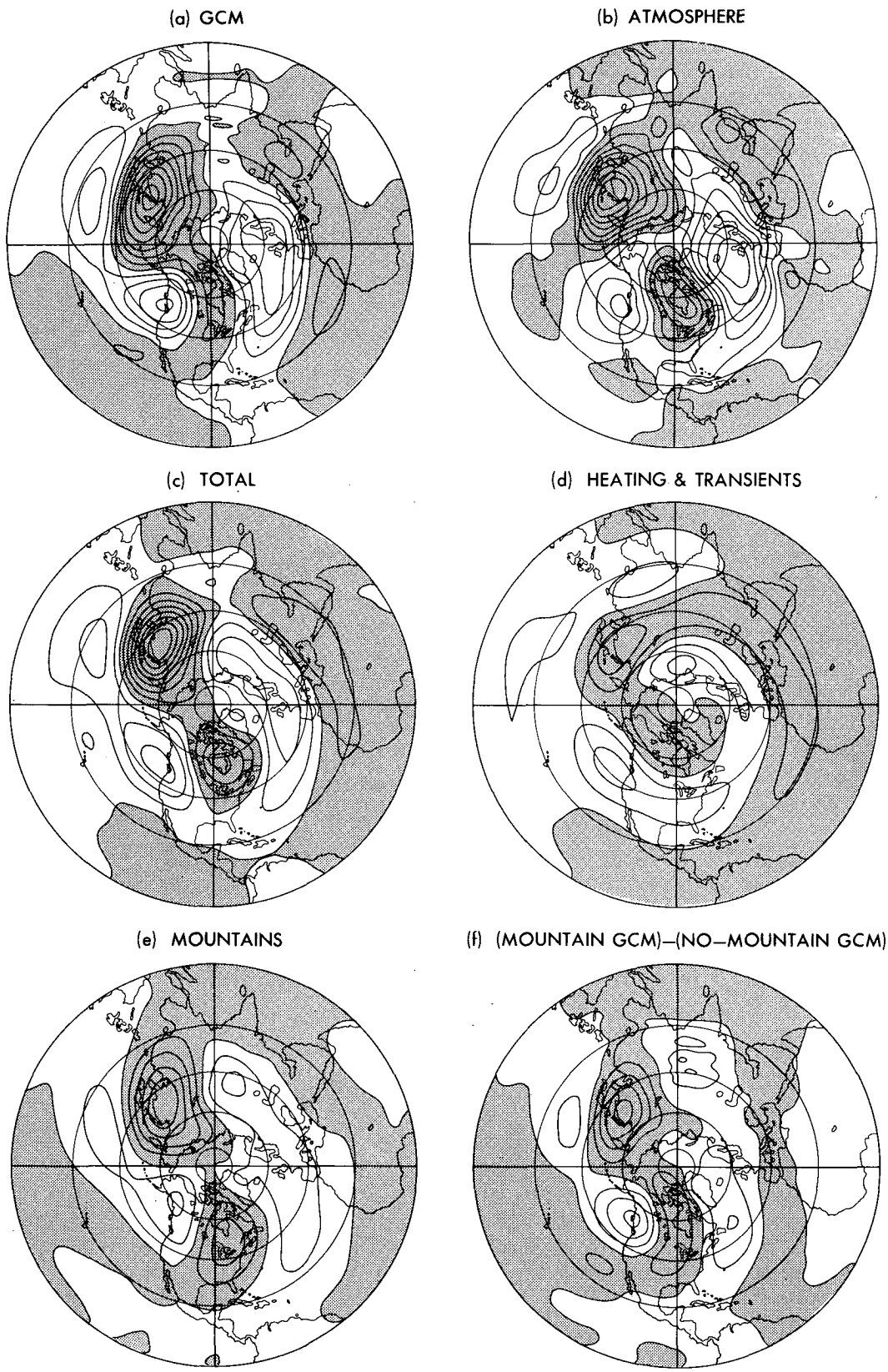

FIG. 5. As in Fig. 3 except for the 300 mb eddy geopotential field which is shown in the northern hemisphere using the polar stereographic projection, and a contour interval of 40 gpm.

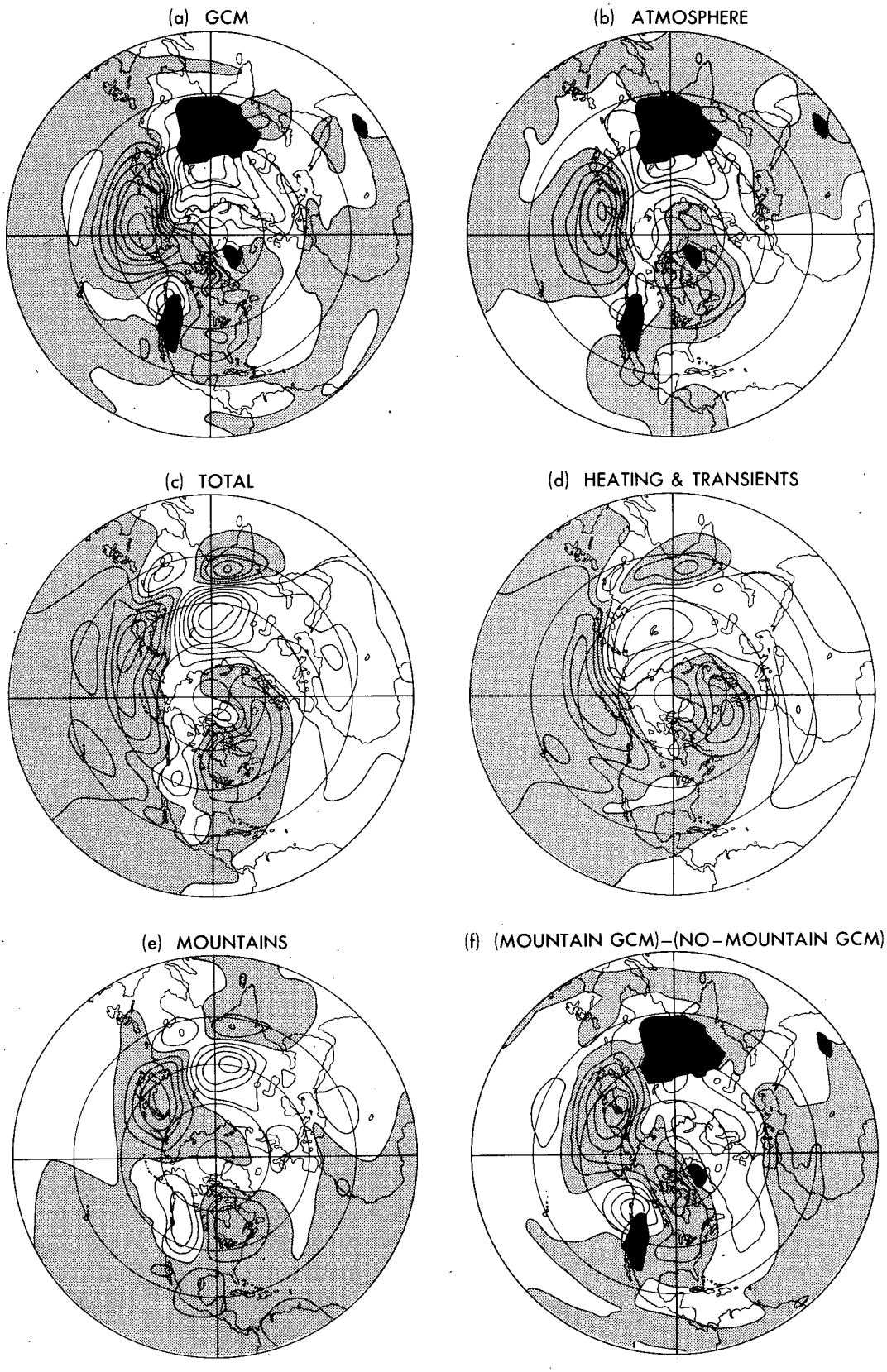

FIG. 6. As in Fig. 5 except for the 900 mb eddy geopotential field; the contour interval is 20 gpm.

for the westward displacement is an exaggerated orographic response. However, comparison with the (Mountain GCM) minus (No-Mountain GCM) difference (Fig. 6f) shows the orographic low in the lee of Tibet to be positioned correctly in the linear simulation; the amplitude of the linear solution is also approximately correct. The linear model implies that orography and heating plus transients contribute about equally to the Siberian high, but Fig. 6f suggests in this case that the orographic contribution is being overestimated. The low off the east coast of North America in the linear model is very similar to the observations (Fig. 6b) but considerably distorted when compared to the GCM.

Although not very clearly shown by the geopotential field, the low-level linear solution becomes noisy and unreliable as one moves into the subtropics. It recovers as one enters the tropics, where its ability to mimick the GCM is as good as in Part I. Overall, the full linear model provides a somewhat less convincing simulation of the GCM in the lower than in the upper troposphere.

Decomposition of the orographically forced solution into parts forced by the orography of eastern and western hemispheres holds no surprises. Figure 7 shows this decomposition for the eddy zonal wind and geopotential at 300 mb. The overlap between the two dominant wavetrains forced by the Himalayan–Tibetan complex and the Rockies is sufficiently small that all of the major highs and lows in the total orographically forced solutions (Fig. 3e and 5e) can be attributed to one or the other of these two sources. Once again, these results are very similar to the analogous barotropic calculations described in Held (1983).

Figure 7 shows rather clearly that in this linear model orographically forced wavetrains are absorbed in the tropics where Rayleigh dissipation is quite large (O[1 day]$^{-1}$). As evident from Fig. 1a, a critical surface (a surface in the latitude–height plane containing critical latitudes) is present only in the lower tropical troposphere ($p > 600$ mb); how baroclinic or equivalent barotropic wavetrains interact with such a surface is not precisely known. Nonetheless, there are no obvious signs of any significant reflection in the steady linear solutions shown in Fig. 7. In barotropic calculations, the critical latitude singularity becomes a near-perfect absorber of Rossby waves when the singularity is removed with linear damping *and* as long as the WKB approximation does not break down away from the critical latitude (Dickinson, 1968). Given the sharp structures in the vorticity gradient needed to produce even modest amounts of reflection in the linear barotropic model examined by Nigam and Held (1983), one does not expect the relatively smooth basic state used here to produce any reflection. Further, a comparison of the linear and GCM solutions does not suggest that significant reflection of the equatorward directed wavetrains would improve the linear simulation, the implication being that little reflection is occurring in the GCM as well; this is consistent with the conclusion of Held (1983) based on computations of the correlation coefficient between U' and V' in the GCM's subtropics. It remains possible that reflection of quasi-stationary waves from the tropics may be important for the low-frequency variability present in the GCM or the atmosphere, and that higher resolution GCMs might show signs of reflection even in their climatologies.

That not all of the difference between the Mountain and the No Mountain GCM is due to direct mechanical orographic forcing is most clearly evident from a comparison of Figs. 3e and 3f. Zonal wind changes in the equatorial Pacific and over North America, in particular, do not seem to be directly related to the orographically forced linear waves. Our attempts to explain these changes in eddy zonal wind as forced by changes in heating and/or transients have not been quantitatively successful. It may very well be that a model linearized about the zonally symmetric flow, and with arbitrary dissipative parameterization is inadequate for this purpose.

4. Contribution of heating and transients

Figure 8 splits the 300 mb response forced by heating plus transients into two parts: the extratropical part is that generated by forcing north of 15°N; the tropical part is that generated by the remainder of the forcing, including all of the Southern Hemisphere forcing. The contour interval for U' (2 m s^{-1}) and ϕ' (20 gpm) are half of those used in Figs. 3 and 5, respectively.

The tropically and the extratropically forced solutions are comparable in amplitude near 30°N; on either side of this latitude, the locally forced solutions prevail. The tropically forced winds are fairly symmetric about the equator, with an $\sim$7 m s^{-1} westerly wind maxima north and south of the Indonesian heating. The remote geopotential response is at most 50 gpm, reaching its maximum value over Alaska and the Rockies. In Fig. 9, the tropical response is split further into parts forced by heating plus transients between longitudes 150°W and the Greenwich meridian (referred to as Amazonian heating) and another due to the forcing in the remaining longitudes (referred to broadly as Indonesian heating). It is evident that it is the Indonesian heating that forces almost all of the 50 gpm response at 300 mb over Alaska and the Rockies (note that the contour interval for the geopotential has been lowered to 10 gpm in Fig. 9).

It is interesting to compare Fig. 9 with Fig. 7 in I, and note that using our frictional parameterization, at least, we find that the introduction of mountains changes only the magnitude of the tropically forced response; both the Amazonian and the Indonesian forced wavetrains enter the northern subtropics with greater amplitudes but have essentially the same ray paths as in I. The Indonesian heating continues to be

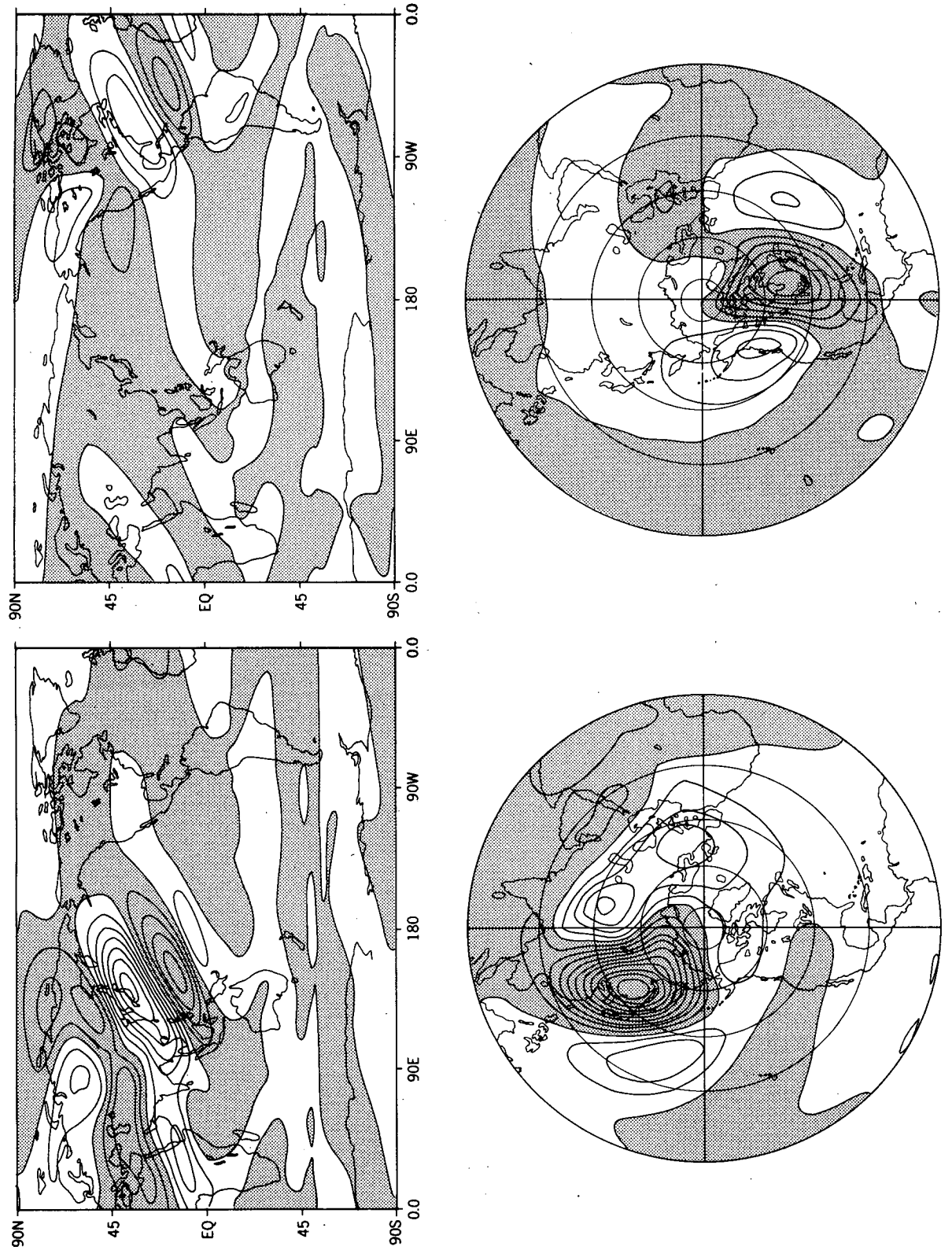

FIG. 7. Decomposition of the orographically forced linear solution at the 300 mb level: the eddy zonal velocity and geopotential forced by the eastern hemisphere orography are shown in the left panel while those forced by the western hemisphere orography are shown in the right hand panel. The contour interval is 2 m s^{-1} for U' and 10 gpm for ϕ', and negative values are shaded as before.

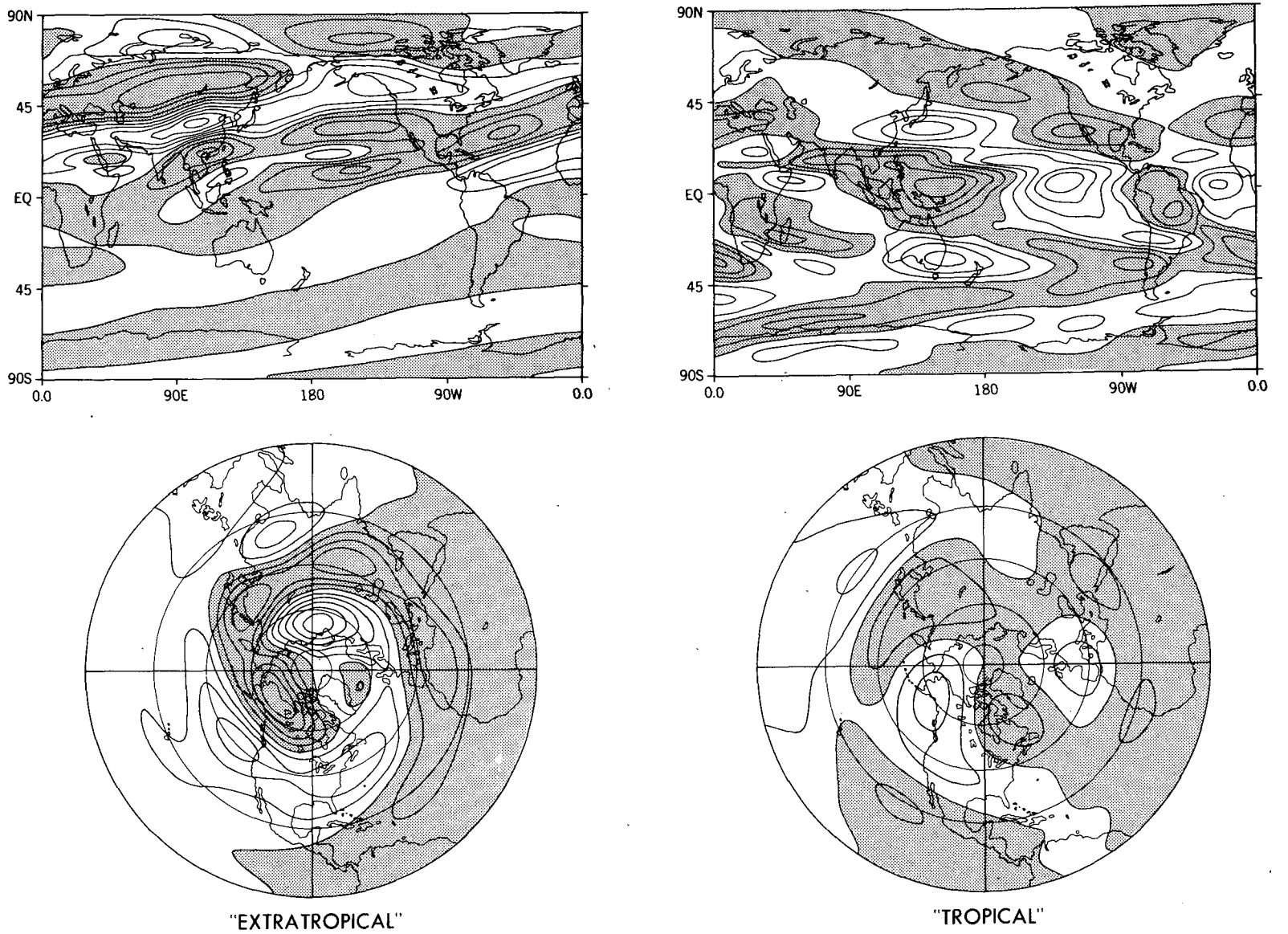

FIG. 8. The 300 mb linear response to heating plus transients is split into two parts: the eddy zonal velocity and geopotential forced by the 'extratropical' ($\theta > 15°$N) part is shown in the left hand panel while those forced by the tropical part ($90°\text{S} < \theta < 15°\text{N}$) are shown in the right hand panel; the contour interval is 2 m s^{-1} for U' and 20 gpm for ϕ', and the contouring convention is the same as before.

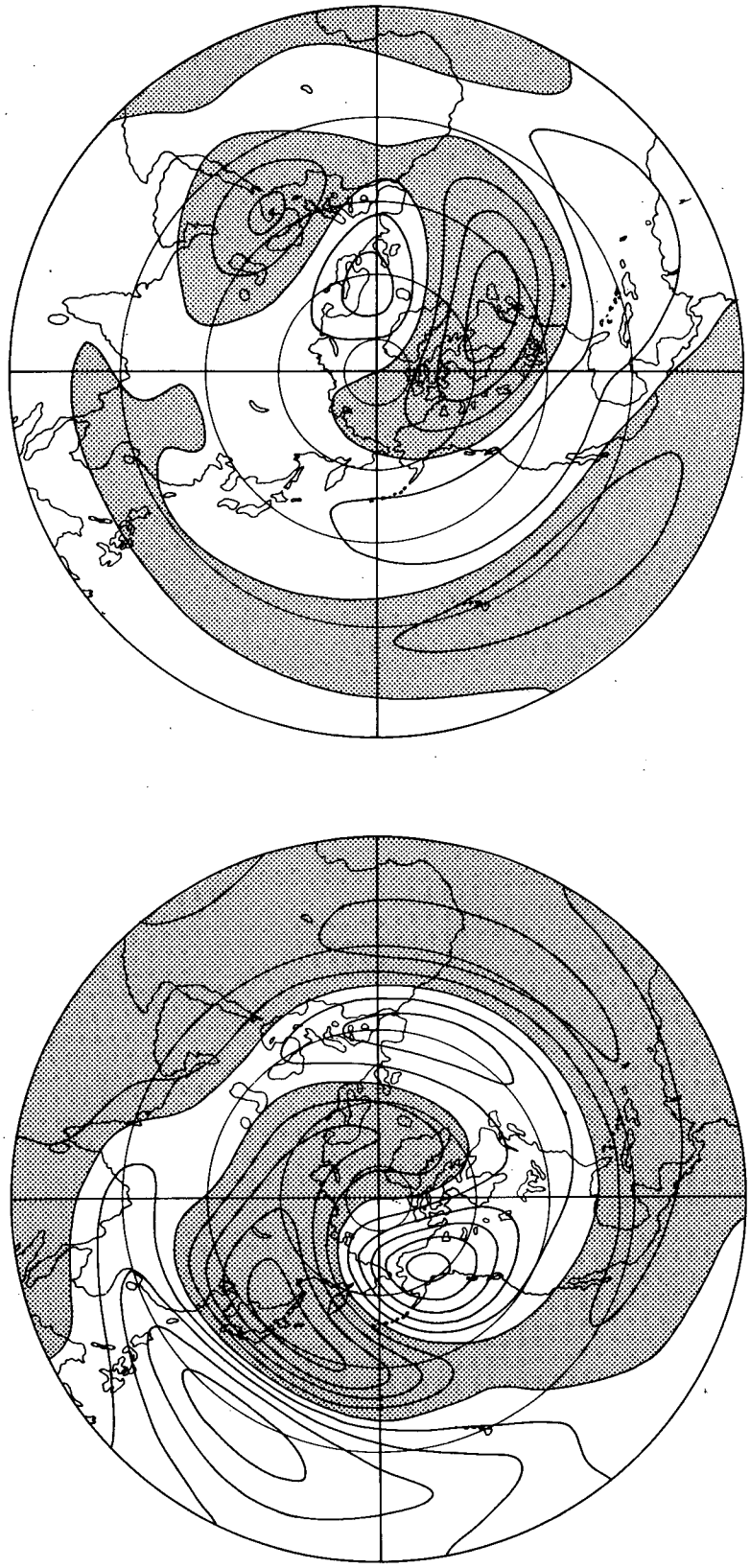

FIG. 9. The tropically forced 300 mb geopotential (of Fig. 8) is split up into parts forced by the 'Indonesian' sector (shown in the left hand panel) and the Amazonian sector (for definition, see the text); the fields are shown in the Northern Hemisphere using a contour interval of 10 gpm which is half of that used in contouring the geopotential in Fig. 8.

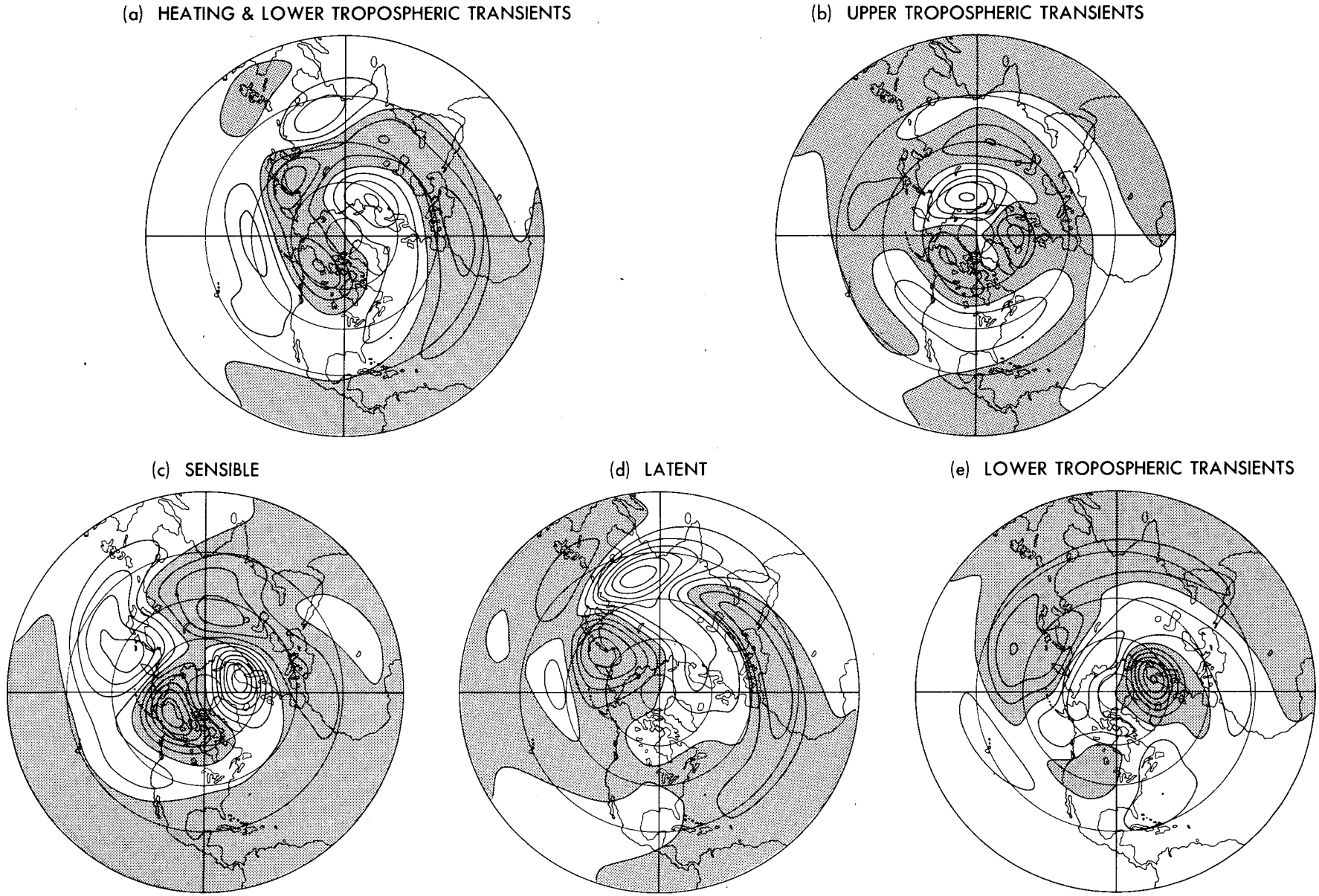

FIG. 10. The 300 mb geopotential response to forcing by 'extratropical' heating plus transients is divided into two parts—the one forced by the upper tropospheric ($\sigma < 0.60$) transients alone is shown in (b). The remaining solution, shown in part (a), is further split into components forced by the total extratropical sensible heating (c), by latent heating (d), and by the lower tropospheric ($\sigma > 0.60$) transients in (e). The contour interval in all these figures is 20 gpm.

dominant, and produces a wavetrain that extends not only across the Pacific but into the Atlantic as well.

The extratropically forced component in Fig. 8 also resembles the analogous result in I, except over southern and eastern Asia. It is this part of the thermally forced solution that causes a deterioration of the full linear simulation (this is clearer when we reduce the contour interval in Fig. 5). As mentioned in section 2, we have substituted the GCM heating rate per unit mass as a function of σ into the linear model, and this introduces significant distortion in the solution over Tibet. This is particularly true because a heating rate that is actually occurring in the midtroposphere of the GCM forces the linear model near 1000 mb where the basic state zonal winds are much weaker. The result is to greatly exaggerate the response, as an air parcel spends more time than it should in the heated region. We have experimented with modifying the Tibetan heating or removing it entirely, but we find that results are sensitive to the details of the procedure used. It also seems that the linear model's response to the southernmost part of the heating in the extratropical storm track off the Asian coast contributes to the poor simulation of the linear waves in this sector.

The 300 mb geopotential response to extratropical forcing is divided further in Fig. 10 into a part forced by the *upper* troposphere transients (sum of thermal and mechanical, and shown in Fig. 10b) and another forced by the full extratropical diabatic heating field and the *lower* tropospheric transients (Fig. 10a); note that the sum of Figs. 10a and 10b is precisely the response to extratropical forcing shown on the left in Fig. 8. Our motivation for this decomposition is partly the feeling that transient mixing in the upper and lower troposphere can usefully be thought of as due to distinct physical mechanisms, and partly because of the close relationship between diabatic heating and lower tropospheric transient eddy heat fluxes evident in Fig. 2. Our definition of the upper troposphere is $\sigma < 0.6$ ($p < 600$ mb).

The upper tropospheric transients are seen to produce a high of 80 gpm over northern Siberia. Comparison of the linear and the GCM solution in Fig. 5 indicates that this high is a significant contributor to the discrepancy between these two; just as in I, we obtain a somewhat better simulation of the GCM by omitting the response to upper tropospheric transients altogether. Why this is so is unclear. Except over Siberia, the 300 mb geopotential response to extratropical heating plus lower tropospheric transients is larger than that forced by the upper tropospheric transients, so Fig. 10a alone resembles the response to extratropical forcing in Fig. 8.

Figure 10 also shows a further decomposition of Fig. 10a into parts forced by sensible heating (Fig. 10c), latent heating (Fig. 10d), and lower tropospheric transients (Fig. 10e). The linear response to the GCM diagnosed radiative heating is negligible, and is therefore not shown. Few features in Fig. 10a can be attributed to either one of the three forcings. The 300 mb geopotential responses to sensible heating and lower tropospheric transients are strongly anticorrelated, particularly off Japan and Scandinavia; sensible heating produces highs in these regions while transients produce lows. The upper-level response to extratropical latent heat release is confined mostly to the eastern hemisphere even though the vertically averaged latent heating of the GCM's atmosphere is considerable over northeastern Pacific and North America (see Fig. 2b); and more often than not, this response is out of phase with that forced by sensible heating. Both of these findings are different from those in I. Some of these differences are due to the distorted response to heating over Tibet and to the intense storm track heating extending to subtropical latitudes off the Chinese coast. The large high produced by latent heating over southeast Asia contributes to the distortion of the full linear simulation. The rather poor linear simulation over northeastern Canada and Hudson Bay appears to be due to the forcing by extratropical diabatic heating plus transients, but it is difficult to identify which component of it is in fact the culprit.

Separation of the effects of lower tropospheric heating and transients strikes us as less than helpful in trying to untangle the underlying dynamics. The compensation becomes even more severe for the lower tropospheric response (not shown), where the southeast Asian heating creates more severe problems. The impression given is that the dynamics is qualitatively similar to that contained in the simple advection–diffusion equation

$$\bar{U}\frac{\partial T'}{\partial X} = F' + D\nabla^2 T'$$

with F' thought of as representing latent plus sensible heating and the diffusion crudely representing transients. If the lowest order balance is, in fact, between the forcing and the diffusive mixing, the linear response to *fixed* heating will not be robust. In particular, it will give a misleading impression as to the sensitivity of the stationary eddies to small changes in the wind field $\bar{U}$, or to changes in other dissipative terms in the model. Thus, the lower tropospheric mixing must be better parameterized to produce a satisfactory linear estimate of the response to lower tropospheric thermal forcing.

5. Sensitivity to thermal and mechanical damping

The amplitude of orographically forced waves in the vicinity of the forcing is not very sensitive to the model damping mechanisms, but, as anticipated, the sensitivity does increase as one follows the wavetrains away from their sources. To illustrate this point, the left panel in Fig. 11 shows the 300 mb perturbation zonal wind and geopotential response to the eastern hemisphere orography when thermal damping of the same form

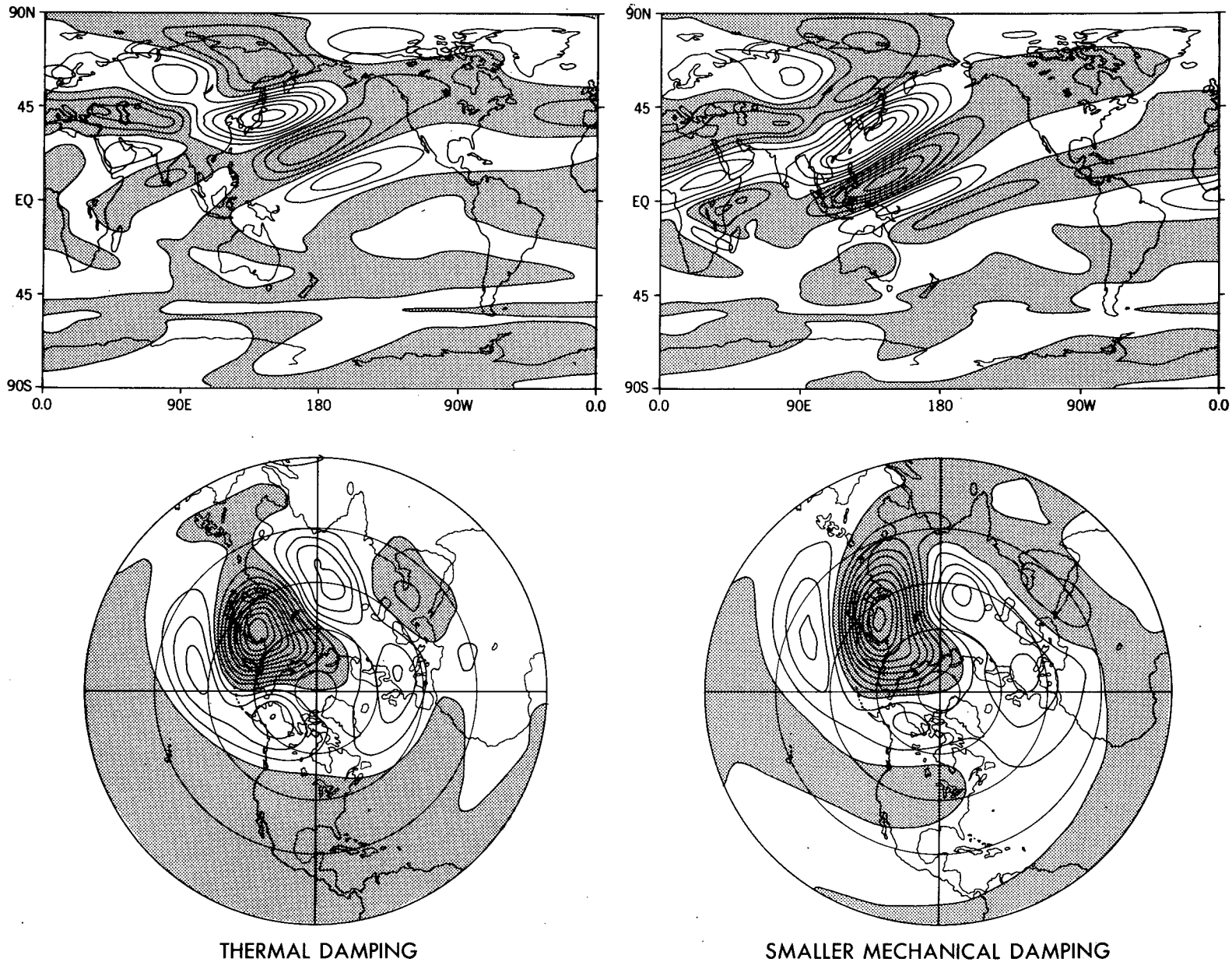

FIG. 11. The 300 mb eddy zonal velocity and geopotential forced by the eastern hemisphere orography, and obtained from the linear model in the presence of thermal damping (of the sort described in the text) are shown in the left-hand panel; those shown in the right hand panel are obtained using a smaller Rayleigh friction in the tropics. Contour interval and convention as in Fig. 7.

as that used in section 6 of I is added to the model: (5 days)$^{-1}$ at the surface decreasing to (20 days)$^{-1}$ at 200 mb. While the amplitude of the dominant low off the Asian coast is not significantly altered, the part of the solution that arcs across the Pacific has increased in strength resulting in a high of nearly 80 gpm over the Gulf of Alaska. As a consequence, there is now considerable overlap between the solutions forced by Tibet and the Rockies. This result may be related to the point made by Held et al. (1986) that thermal damping can cause the amplitude of a stationary external Rossby wavetrain to increase in the direction of its group velocity. We do not think of this thermal damping as a good parameterization of mixing by transients, but the calculation does illustrate the potential sensitivity of the orographically forced waves to such damping.

We show in the right panel of Fig. 11 the perturbation zonal wind and geopotential forced by the eastern hemisphere orography when the strength of tropical damping is reduced from a maximum of (1.5 days)$^{-1}$ to (10 days)$^{-1}$. The result is simply that the wave penetrates more deeply into the tropics as is particularly evident in the zonal wind field. We find that this deeper penetration does not help in producing a better simulation of the GCM's flow since the resulting zonal wind field has too much meridional structure. For reasons that are not clear, the zonal wind response over Africa to the orographic forcing is quite sensitive to both thermal and mechanical damping in this model.

As expected from the results in I, the tropical response to tropical heating is very sensitive to the local Rayleigh friction. Figure 12 shows the 300 mb zonal wind and geopotential forced by tropical heating plus transients when tropical damping is reduced as described above. Comparison with Fig. 8 shows winds along the equator to be much stronger now, in clear disagreement with the GCM; the changes in the extratropics are however comparatively modest. When the linear model is forced by tropical diabatic heating alone (i.e., without any transient eddy flux convergences), the tropical and extratropical responses are somewhat larger ($\sim$20%) because tropical thermal transients act to reduce the amplitude of tropical diabatic heating (see Fig. 2). The linear simulation of the total extratropical height field is however much less sensitive to such details because of the dominance of orographic forcing.

6. Discussion and conclusions

We find linear theory to be useful in explaining qualitatively and quantitatively the wintertime circulation obtained in a GCM with realistic orography, despite the fact that the dissipative terms added to the model are quite arbitrary. Our choices in this regard may not be optimal. In fact, further calculations suggest that the correspondence between linear model and GCM can be improved somewhat by replacing some of the Rayleigh friction in the tropics with diffusion and increasing the damping in midlatitudes. However, there is little reason to believe that the best scheme for simulating this particular GCM will also be best for other models, and so we have not tried to tune the model further. Theoretical guidance is clearly needed.

The orographic component of the linear model's stationary wave patterns is relatively insensitive to dissipation, although the sensitivity does increase as one follows the dominant ray paths downstream. There is little overlap between the two principal orographically forced wavetrains emanating from Tibet and the Rockies. These wavetrains are absorbed as they enter the tropics in the linear model and, as best we can tell, in the GCM as well. We see no clear indications that our simulation of the GCM would be improved if some reflection were to occur in the linear model.

The relative contribution of orography to the total upper tropospheric circulation is different for different dynamical fields. Orography forces about half of the 300 mb eddy zonal velocity, two-thirds of the 300 mb eddy geopotential, and an even larger fraction of the eddy meridional velocity field. Orography is dominant in the fields that highlight shorter zonal scales (i.e., zonally propagating Rossby waves).

In the lower troposphere, the response to heating plus transients increases in importance, but the orographic response still contributes nearly 50% to the 900 mb geopotential field in our decomposition. However, the linear model's simulation of the total eddy field is less convincing in the lower than in the upper troposphere.

Midlatitude orography affects the tropical as well as the extratropical flow. Wavetrains forced by Tibet and the Rockies penetrate into the western tropical oceans, where they contribute as much to the eddy zonal velocities as do tropical thermal forcings. Having eliminated Antarctica from the linear model, the response to orography is very small in the Southern Hemisphere, even near the Andes.

The linear response to orography provides a surprisingly good simulation of the difference in the eddy geopotential between the Mountain and No-mountain GCMs, although there are some interesting differences in the dominant ray paths. Much larger discrepancies are evident in the eddy zonal velocities. Since thermal forcing contributes substantially to the long zonal length scales that stand out in the U' pattern, it seems plausible that differences in the U' field are created by differences in the thermal (or transient) forcing between the two GCM's, rather than by nonlinearity of the orographic response itself. However, the inclusion of these differences in the linear model does not significantly improve the simulation.

We divide the forcing by heating plus transients into a tropical and an extratropical part, as in I. The remote response to tropical forcing is largest over Alaska and western North America, but only reaches 50 gpm at 300 mb. This remote signal is mostly the response to

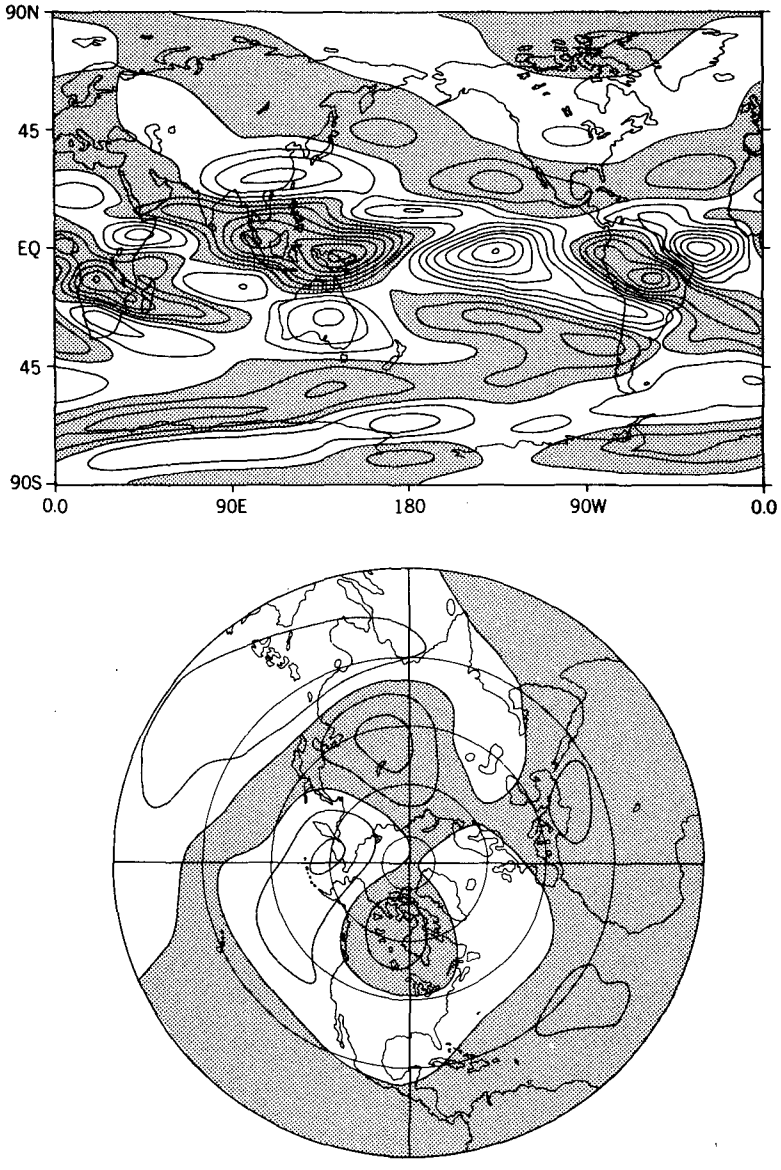

FIG. 12. The tropically forced 300 mb eddy zonal velocity and geopotential, obtained using smaller Rayleigh friction in the tropics. Contour interval and convention as in Fig. 8.

heating over Indonesia and the Western Pacific. The large zonal scale of this part of the tropical heating is evidently important in generating a wavetrain that penetrates further into high latitudes than that generated by the intense, but more localized Amazonian heating.

The response to extratropical heating plus transients is very different from that found in I over Southeast Asia, but elsewhere there is considerable similarity (compare the geopotential in the left panel of Fig. 8 with Fig. 6b in I). The full linear model does not provide a good simulation over Southeast Asia; it seems to be distorting the response over the Tibetan plateau and the southernmost part of storm track heating, which happens to be near the low-level critical latitude.

Because of considerable cancellation in high latitudes between the upper tropospheric responses forced by the transients and sensible heating, we do not believe that these individual responses are very meaningful. But, if one does sum Figs. 10b and 10e to compute the total response of this linear model to thermal and mechanical transients, the result is modest, with geopotential amplitudes of 100 gpm only in higher latitudes. This result is at variance with conclusions of some earlier investigations of the importance of transient forcing. In particular, Opsteegh and Vernekar (1982) find the transient contribution to the 400 mb geopotential to be comparable to, if not larger than, the combined contributions of orography and diabatic heating. As shown in Lau and Nath (1987), our GCM's storm

tracks are somewhat weaker than those observed; also the eddy momentum fluxes in the subtropics are known to be deficient. A similar calculation for a higher resolution GCM could very well produce a significantly larger response to transient forcing.

As in I, our results show the transients to be very important for the low-level response. We have not shown the decomposition of the 900 mb response to heating plus transients (Fig. 6d) into its separate components because the cancellations that one finds are even more extreme than in I. The effect of extratropical lower tropospheric transients on the eddy temperature field is at least in part akin to that of diffusive mixing.

Despite some notable weaknesses, particularly in the vicinity of tropical critical latitudes, and despite the arbitrariness of the tropical damping needed to obtain realistic eddy zonal velocities near the equator, the linear model proves to be a useful tool in interpreting the GCM. Much remains to be understood about the behavior of such models and their reliability, but it is clear that they can take us only part way to a satisfying theory of the stationary eddies. Future tasks must include the development of steady nonlinear models and studies of the feedback between the stationary eddies and the thermal and transient forcing.

Acknowledgments. A preliminary version of this work constitutes part of the Ph.D. thesis of S. Nigam in the Geophysical Fluid Dynamics Program at Princeton University. We would like to thank S. Manabe, N.-C. Lau, K. Miyakoda, and R. S. Lindzen for helpful discussions on this topic, and A. H. Oort for providing the data for Figs. 3–6. The figures were expertly drafted by the Scientific Illustration Group at GFDL. S. Nigam has been supported at MIT by NASA Grant NAGW-525 and NSF Grants ATM 8342482 and 8520354.

REFERENCES

Blackmon, M. L., G. W. Branstator, G. T. Bates and J. E. Geisler, 1987: An analysis of equatorial Pacific sea surface temperature anomaly experiments in General Circulation models with and without mountains. *J. Atmos. Sci.*, **44,** 1828–1844.

Charney, J., and A. Eliassen, 1949: A numerical method for predicting the perturbations of the middle latitude westerlies. *Tellus,* **1,** 38–54.

Dickinson, R. E., 1968: Planetary Rossby waves propagating vertically through weak westerly wind wave guides. *J. Atmos. Sci.*, **25,** 984–1002.

Held, I. M., 1983: Stationary and quasi-stationary eddies in the extratropical troposphere: Theory. Large-scale Dynamical Processes in the Atmosphere, Eds. B. J. Hoskins and R. P. Pearce, Academic Press, 127–167.

——, R. L. Panetta and R. T. Pierrehumbert, 1985: Stationary external Rossby waves in vertical shear. *J. Atmos. Sci.*, **42,** 865–883.

——, R. T. Pierrehumbert and R. L. Panetta, 1986: Dissipative destabilization of external Rossby waves. *J. Atmos. Sci.*, **43,** 388–396.

Hendon, H. H., and D. L. Hartmann, 1982: Stationary waves on a sphere: Sensitivity to thermal feedback. *J. Atmos. Sci.*, **39,** 1906–1920.

Hoskins, B. J., and D. J. Karoly, 1981: The steady linear response of a spherical atmosphere to thermal and orographic forcing. *J. Atmos. Sci.*, **38,** 1179–1196.

Jacqmin, D., and R. S. Lindzen, 1985: The causation and sensitivity of the Northern winter planetary waves. *J. Atmos. Sci.*, **42,** 724–745.

Johnson, D. R., R. D. Townsend and M.-Y. Wei, 1985: The thermally coupled response of the planetary scale circulation to the global distribution of heat sources and sinks. *Tellus,* **37A,** 106–125.

Kalnay, E., K. C. Mo and J. Paegle, 1986: Large-amplitude, short-scale stationary Rossby waves in the Southern Hemisphere: Observations and mechanistic experiments to determine their origin. *J. Atmos. Sci.*, **43,** 252–275.

Kasahara, A., and W. M. Washington, 1971: General circulation experiments with a six-layer NCAR model, including orography, cloudiness and surface temperature calculations. *J. Atmos. Sci.*, **28,** 657–701.

Lau, N.-C., 1983: Mid-latitude wintertime circulation anomalies appearing in a 15-year GCM experiment. *Large-Scale Dynamical Processes in the Atmosphere.* B. J. Hoskins and R. P. Pearce Eds., Academic Press, 111–125.

Lau, N.-C., and A. H. Oort, 1981: A comparative study of observed Northern Hemisphere circulation statistics based on GFDL and NMC analyses. Part I: The time-mean fields. *Mon. Wea. Rev.*, **109,** 1380–1403.

Lau, N.-C., and M. J. Nath, 1987: Frequency dependence of the structure and temporal development of wintertime tropospheric fluctuations—comparison of a GCM simulation with observations. *Mon. Wea. Rev.*, **115,** 251–271.

Lin, B.-D., 1982: The behavior of winter stationary planetary waves forced by topography and diabatic heating. *J. Atmos. Sci.*, **39,** 1206–1226.

Manabe, S., and T. B. Terpstra, 1974: The effects of mountains on the general circulation of the atmosphere as identified by numerical experiments. *J. Atmos. Sci.*, **31,** 3–42.

Newell, R. E., J. W. Kidson, D. G. Vincent and G. J. Boer, 1972, 1974: *The General Circulation of the Tropical Atmosphere.* The MIT Press, 2 Vols. 258 (371) pp.

Nigam, S., 1983: On the structure and forcing of tropospheric stationary waves. Ph.D. thesis, Princeton University.

——, and I. M. Held, 1983: The influence of a critical latitude on topographically forced stationary waves in a barotropic model. *J. Atmos. Sci.*, **40,** 2610–2622.

——, I. M. Held and S. W. Lyons, 1986: Linear simulation of the stationary eddies in a GCM. Part I: The "No Mountain" Model. *J. Atmos. Sci.*, **43,** 2944–2961.

Oort, A. H., 1983: Global Atmospheric Circulation Statistics, 1958–1973: NOAA Prof. Paper No. 14. U.S. Govt. Printing Office, Washington, DC 20402.

Opsteegh, J. D., and A. D. Vernekar, 1982: A simulation of the January standing wave pattern including the effects of transient eddies. *J. Atmos. Sci.*, **39,** 734–744.

Rong-hui, H., and K. Gambo, 1982: The response of a hemispheric multi-level model atmosphere to forcing by topography and stationary heat sources. I: Forcing by topography. *J. Meteor. Soc. Japan,* **60,** 78–92.

Simmons, A. J., 1982: The forcing of stationary wave motions by tropical diabatic heating. *Quart. J. Roy. Met. Soc.*, **108,** 503–534.

Smagorinsky, J., 1953: The dynamical influence of large-scale heat sources and sinks on the quasi-stationary mean motions of the atmosphere. *Quart. J. Roy. Met. Soc.*, **79,** 342–366.

Sutcliffe, R. C., 1951: Mean upper contour patterns of the northern hemisphere—the thermal-synoptic view-point. *Quart. J. Roy. Met. Soc.*, **77,** 435–440.

Tokioka, T., and A. Noda, 1986: Effects of large scale orography on January atmospheric circulation: A numerical experiment. *J. Meteor. Soc. Japan,* **64,** 819–839.

Webster, P. J., 1982: Seasonality in the local and remote atmospheric response to sea surface temperature anomalies. *J. Atmos. Sci.*, **39,** 41–52.

Youngblut, C. E., and T. Sasamori, 1980: The nonlinear effects of transient and stationary eddies on the mean winter circulation. Part I: The diagnostic analysis. *J. Atmos. Sci.*, **37,** 1944–1957.